Brownian colloids in underdamped and overdamped regimes with nonhomogeneous temperature

J. M. Sancho

Universitat de Barcelona, Departament d'Estructura i Constituents de la Matèria, Martí i Franqués, 1, 08028 Barcelona, Spain

(Received 3 July 2015; revised manuscript received 14 September 2015; published 4 December 2015)

The motion of Brownian particles when temperature is spatially dependent is studied by stochastic simulations and theoretical analysis. Nonequilibrium steady probability distributions $P_{st}(z,v)$ for both underdamped and overdamped regimes are analyzed. The existence of local kinetic energy equipartition theorem is also discussed. The transition between both regimes is characterized by a dimensionless friction parameter. This study is applied to three physical systems of colloidal particles.

DOI: 10.1103/PhysRevE.92.062110 PACS number(s): 05.40.−a, 02.50.−r

I. INTRODUCTION

Since their formulation Langevin equations have been a widely accepted paradigm in the studies of Brownian particles motion. These equations fulfill the Boltzmann equilibrium statistics and incorporate interesting nonequilibrium aspects. Nevertheless with a temperature gradient, a clear nonequilibrium situation, the standard form of the Langevin equation needed some revisions due to the presence of multiplicative white noise. This problem was already studied in the 1980s and appropriate Fokker-Planck [1–3] and Langevin equations were derived [2].

In this decade the experimental capability to observe and control the motion of small particles [4] (biomolecules, colloids, etc.) has renewed the theoretical interest for these type of studies [5,6]. Recent experiments of colloidal particles under nonhomogeneous friction [7,8], or temperature gradient [9,10] raised a high incremental interest in this topic [11–20]. Although the Brownian motion of noninteracting particles is a simple system, it still presents interesting theoretical [5,6], experimental [4,7,8,13,14], and stochastic simulation challenges [11,12,20,21].

As the reference equations, either Fokker-Planck or Langevin, cannot be solved analytically for most of the interesting cases, the relevant information has to be extracted from stochastic simulations of the Langevin equations [11,18,20]. In particular the problem of the stochastic interpretations used in the simulations of the Langevin equation has to be addressed. Nevertheless, as it is well known that the Fokker-Planck associated to the Langevin equations for the two variables (x,v) does not depend on any stochastic interpretation, then one can assume that the Itô interpretation can be justified as an optimal choice for its numerical simplicity. Moreover, other interpretations are equally correct within the appropriate changes.

Brownian particles can exhibit two well-separated dynamical regimes, underdamped and overdamped, as a function of the friction parameter that we will assume to be constant. Here we will address the study of free Brownian particles under a temperature gradient and for these two different regimes. The main specific topics under the focus of this paper are the steady nonequilibrium distributions and the existence of the local equipartition energy theorem in both underdamped and overdamped regimes.

The outline of the paper goes as follows. In the next section we will discuss the relation between Fokker-Planck (FP) equations, Langevin equations, and numerical simulations according to the Itô interpretation. The possible existence of analytical expressions for the steady distributions is also analyzed. Specifically, a practical criteria to discriminate these underdamped and overdamped regimes is derived. In the third section we study several models of colloids with experimental relevance where the steady distributions, and the local kinetic energy equipartition theorem are checked numerically. We end with a discussion and the summary of the main conclusions.

II. LANGEVIN AND FOKKER-PLANCK EQUATIONS

A. Definitions and algorithms

Let us start with the generic situation described by the Langevin equation for noninteracting classical Brownian particles,

$$\ddot{z} = -\hat{\gamma}_0 \dot{z} - V'(z) + g(z)\xi(\tau), \tag{1}$$

where $V(z)$ is an external potential and $\xi(\tau)$ is the thermal Gaussian white noise with zero mean and correlation $\langle \xi(\tau)\,\xi(\tau')\rangle = 2\delta(\tau - \tau')$. All variables and parameters have been rescaled to be dimensionless [22]. The interesting situation here is the fact that temperature $\hat{T}(z)$ is spatially dependent, with the following local fluctuation dissipation relation,

$$g(z)^2 = \hat{\gamma}_0 \hat{T}(z). \tag{2}$$

Here we will assume that friction $\hat{\gamma}_0$ is constant along the spatial domain. The general case of a nonconstant friction is discussed in Sec. V. This relation (2) is a standard assumption on Brownian motion studies [2,5–20]. It will be analyzed how this relation affects the local kinetic energy equipartition theorem in both underdamped and overdamped regimes.

It is worth emphasizing that the multiplicative noise function $g(z)$ appears in the second-order differential equation (1). Then, it is an exercise to prove that the corresponding Fokker-Planck (FP) equation for the probability density $P(z,v;\tau)$ does not depend on any stochastic interpretation of the term $g(z)\xi(\tau)$. It reads,

$$\frac{\partial P(z,v;\tau)}{\partial \tau} = -\frac{\partial}{\partial z} vP + \frac{\partial}{\partial v}[\hat{\gamma}_0 v + V'(z)]P + \frac{\partial^2}{\partial v^2} g(z)^2 P. \tag{3}$$

The numerical simulation of Eq. (1) is standard and the following predictor-corrector algorithm has been used:

$$\begin{aligned}\bar{z} &= z_\tau + v_\tau \Delta\tau,\\ \bar{v} &= v_\tau - \gamma_0 v_\tau \Delta\tau - V'(z_\tau)\Delta\tau + g(z_\tau)\chi(\tau),\end{aligned} \tag{4}$$

$$\begin{aligned}z(\tau+\Delta\tau) &= z_\tau + (v_\tau + \bar{v})\frac{\Delta\tau}{2},\\ v(\tau+\Delta\tau) &= v_\tau - \gamma_0[v_\tau + \bar{v}]\frac{\Delta\tau}{2}\\ &\quad + [V'(z_\tau) + V'(\bar{z})]\frac{\Delta\tau}{2} + g(z_\tau)\chi(\tau),\end{aligned} \tag{5}$$

with the simplified notation, $z(\tau) \equiv z_\tau$ and $v(\tau) \equiv v_\tau$. $\chi(\tau)$ is a random process

$$\chi(\tau) = \sqrt{2\Delta\tau}\ \eta_\tau, \tag{6}$$

where η_τ are Gaussian random numbers $N(0,1)$ generated at each time step. The former algorithm is the well-known Heun scheme [23]).

The first two equations correspond to the predictor part and the last two are the corrector part. The stochastic interpretation appears as Itô in both predictor and corrector parts because it is the simplest choice, given the independence of the stochastic interpretation, and that the algorithm is explicit. Moreover, in order to warrant the equivalence of this numerical algorithm with the Fokker-Planck equation (3) the time step Δt should be the smallest time scale of the system.

B. Overdamped regime

The former Langevin equation (1) describes both underdamped and overdamped regimes. As we have seen there is no problem with the interpretation of it. Nevertheless important and controversial problems appear when one wants to write the overdamped limit Langevin equation corresponding to (1)–(2). In this limit the velocity (faster) variable has to be eliminated adiabatically from the the full inertial Langevin equation (1). This was carried out following rigorous mathematical procedures in Refs. [1,2] and recently rederived in Refs. [6,17–19]. The key point is an expansion in the $\hat{\gamma}_0$ as a large quantity, which leads to the overdamped limit approximation. This is manifest in the final form of the Fokker-Planck equation, which is of order $\hat{\gamma}_0^{-1}$ in the drift and diffusion terms,

$$\frac{\partial P^o(z;\tau)}{\partial \tau} = \frac{\partial}{\partial z}\frac{1}{\hat{\gamma}_0}\left[V'(z) + \frac{\partial}{\partial z}\hat{T}(z)\right]P^o(z;\tau), \tag{7}$$

where the superscript "o" means overdamped.

This singular perturbation calculation cannot be passed over by the shortcut of putting the acceleration (or the particles mass) equal to zero.

C. Steady states

The steady probability distribution $P_{st}(z,v)$ is only known in an equilibrium situation [$\hat{T}(z) = \hat{T}_0$] and it is the Boltzmann one,

$$P_{st}(z,v) \sim \exp\left[-\frac{v^2/2 + V(z)}{\hat{T}_0}\right], \tag{8}$$

which is independent of an inhomogeneous or constant friction. Under a nonconstant temperature the steady distribution is not known [17].

Nevertheless the steady distribution in the overdamped limit (7) is the quadrature,

$$P^o_{st}(z) = \frac{N}{\hat{T}(z)}\exp\left(-\int^z \frac{V'(z')}{\hat{T}(z')}dz'\right), \tag{9}$$

where N has to be obtained from normalization.

From this partial information we will first propose a weak solution of the overdamped regime and explore its domain of validity. The proposal is composed of two steady distributions,

$$P^o_{st}(z,v) = P_{st}[v,\hat{T}(z)]P^o_{st}(z), \tag{10}$$

where $P_{st}[v,\hat{T}(z)]$ is the local Maxwellian distribution,

$$P^o_{st}[v,\hat{T}(z)] = \frac{1}{\sqrt{2\pi\hat{T}(z)}}\exp\left(-\frac{v^2}{2\hat{T}(z)}\right). \tag{11}$$

This proposal fulfills two important conditions,

$$P^o_{st}(z) = \int P^o_{st}(z,v)dv, \tag{12}$$

and the local energy equipartition theorem in terms of the local temperature,

$$\langle v^2(z)\rangle_{st} = \int v^2 P^o_{st}[v,\hat{T}(z)]dv = \hat{T}(z). \tag{13}$$

Moreover, this theorem, well accepted for overdamped cases, will merit a numerical check of its domain of validity for both underdamped and overdamped regimes.

By a direct substitution of (10) in (3) one can check that the weak solution (10) could obey the the FP equation (3) if the following condition would be satisfied,

$$3v\ P^o_{st}(z,v) = \frac{v^3}{\hat{T}(z)}P^o_{st}(z,v). \tag{14}$$

This condition is not fulfilled but with the Gaussian approximation for the nonlinear term $v^3 \sim 3v\langle v^2\rangle = 3v\hat{T}(z)$, it holds. Nevertheless, the solution (10) will be tested by numerical simulations. Specifically, we will check the domain of validity of the steady distributions $P^o_{st}(z)$ (9) and $P^o_{st}[v,\hat{T}(z)]$ (11).

D. Criteria for underdamped and overdamped regimes

Random motion in fluids present two different dynamical regimes depending on whether or not the inertia dominates. The Reynolds number determines the separation of these two regimes in terms of the physical quantities: fluid density (ρ), characteristic particle length (l) and velocity (v), and the dynamical viscosity (η). Nevertheless, in the scenario of Brownian particles other physical quantities are involved. Here we address this problem for Brownian particles described by the Langevin equation (1) when friction is constant.

In the underdamped regime the Langevin equation of motion (1) takes the form $\dot{v} = -\hat{\gamma}_0 v + \cdots$ and the velocity relaxes with the function $\sim e^{-\hat{\gamma}_0\tau}$ so the time scale is $\tau_v = \hat{\gamma}_0^{-1}$. Nevertheless, in the overdamped regime we have no inertia term and the equation of motion takes the form of $\hat{\gamma}_0 dx/d\tau = \ldots$, and friction $\hat{\gamma}_0$ can be absorbed in a new τ variable measured in units of $\hat{\gamma}_0$, which gives a characteristic time

$\tau_z = \hat{\gamma}_0$. The separation between these regimes will appear when these two times are equal,

$$\hat{\gamma}_0 = 1. \tag{15}$$

This condition will be checked by simulations. As $\hat{\gamma}_0$ is a dimensionless parameter it has to be expressed in terms of the physical parameters of the model under study. If friction is nonconstant, the criteria have to be applied locally.

E. Numerical details and observables

A finite z variable domain $[0,10]$ is fixed, with reflecting boundary conditions, divided in 40 bins of size $\Delta z = 0.250$ and the v domain $(-5,5)$ in 40 bins of size $\Delta v = 0.250$. We have used $N = 160\,000$ particles, which is enough to achieve our objectives.

The initial distribution is $P(z,v;0) = P(z;0)P(v;0)$, where $P(z;0)$ is constant in the interval $z\ \varepsilon\ [3,7]$ and $P(v;0)$ is a Maxwellian distribution with a temperature $T_0 = 0.1$. This initial distribution is far from any possible steady distribution.

Numerical simulations were conducted using the algorithm (4)–(5) up to a maximum time,

$$\tau_{\max} \geqslant 5 \times \max\left(\hat{\gamma}_0, \hat{\gamma}_0^{-1}\right), \tag{16}$$

to warrant the achievement of the steady state. According the theoretical points discussed in the introduction, the numerical simulations of the Langevin equations are performed using the Itô prescription with $\Delta\tau$ as the smaller time scale of the system,

$$\Delta\tau \leqslant 0.01 \times \min\left(\hat{\gamma}_0, \hat{\gamma}_0^{-1}\right). \tag{17}$$

Several observables have been recorded: coordinates of (z_i, v_i) for each particle and the distribution $P(z_i, v_j; \tau)$. With this information we have evaluated the reduced distributions $P(z;\tau)$ and $P(v,\tau)$ and the statistical moments of z and v.

Another important quantity is the distance between the simulation distributions and the theoretical expectations. The distance between the steady overdamped distribution (9) and the numerical values $P(z,\tau_{\max})$ is defined as,

$$DIS(Pz) = \int \left| P(z;\tau_{\max}) - P^o_{st}(z) \right| dz, \tag{18}$$

and the distance with respect the local equipartition energy theorem,

$$DIS(FDT) = \int |\langle v^2(\tau_{\max})\rangle_z - T(z)| dz, \tag{19}$$

are recorded and analyzed in the discussion section.

III. RESULTS

In this section three different models of colloidal particles are studied under a linear temperature gradient. The first model is a free Brownian particle, the second is a silica bead in an optical trap, and the last one is a particle in a two wells potential. These cases correspond to standard experimental setups.

A. Free particle

The particle follows the Langevin equation,

$$m\ddot{x} = -\gamma_0 \dot{x} + \sqrt{\gamma_0 k_B T_0 \hat{T}(x/x_0)}\, \eta(t), \tag{20}$$

in terms on physical dimensional parameters and a Gaussian white noise with correlation $\langle \eta(t)\, \eta(t')\rangle = 2\delta(t - t')$. Now we proceed with the adimensionalization of the model. Rescaling the time and space (t,x) to the dimensionless variables (τ,z) by the changes,

$$x = x_0 z, \quad t = t_0 \tau = \sqrt{\frac{m x_0^2}{k_B T_0}}\, \tau, \tag{21}$$

Eq. (20) transforms into,

$$\ddot{z} = -\hat{\gamma}_0 \dot{z} + \sqrt{\hat{\gamma}_0 \hat{T}(z)} \xi(\tau). \tag{22}$$

It has the generic dimensionless structure of (1). The new dimensionless friction is,

$$\hat{\gamma}_0 = \gamma_0 \sqrt{\frac{x_0^2}{m k_B T_0}}. \tag{23}$$

From now on we will take the following spatial dependence for $\hat{T}(z)$,

$$\hat{T}(z) = 1 + 0.1z, \tag{24}$$

in the spatial domain $z \in [0,10]$. There is a factor of two between left and right temperatures. This gradient is not small from experimental point of view of colloidal particles.

The only free parameter is $\hat{\gamma}_0$, which will be used to control the underdamped and overdamped regimes. This parameter is dimensionless and related with the physical parameters of the model (23).

For this model the nonequilibrium overdamped steady distribution (9) is,

$$P^o_{st}(z) = \frac{N}{\hat{T}(z)} = \frac{0.144}{1 + 0.1z}, \tag{25}$$

Our objective is to check this solution, and the local energy equipartition theorem (13) in both underdamped and overdamped regimes.

We will start first by checking the steady probability in this limit. In Fig. 1(a) we see that for $\hat{\gamma}_0 = 6$ we get a perfect agreement between simulation and the theoretical prediction. In this regime the velocity fulfills the local equilibrium condition $\langle v^2(z)\rangle = \hat{T}(z)$ [Fig. 1(b)]. Thus one can conclude that even for not very large friction values, we are in the overdamped regime with predictions (11) and (25).

Moreover, we see also, in these two figures, how the simulation points move to a very different behavior for smaller values of the friction. The slope of $P_{st}(z)$ decreases with $\hat{\gamma}_0$ until the limit of a constant steady distribution $P^o_{st}(z) = 1/10$.

For the velocity steady distribution the analysis of the statistical moments [Fig. 1(b)] show as before that $\langle v^2(z)\rangle$ deviate from the local equilibrium condition. In fact, one can guest from these data, that particles are feeling the mean temperature $\langle \hat{T}\rangle = 1.5$, with the Maxwellian

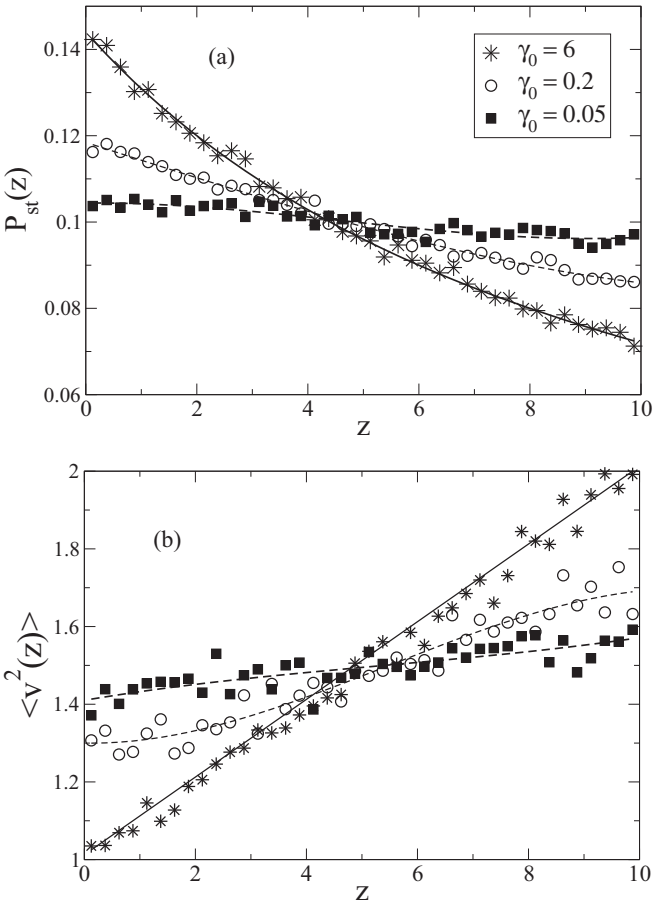

FIG. 1. (a) Simulation results of the steady distribution $P_{st}(z)$ for different values of $\hat{\gamma}_0$ (see inset). Simulation data (symbols). Continuous line is the analytical expression (25). (b) Local second moment $\langle v^2(z)\rangle$ for the values of previous figure. Continuous line corresponds to the energy equipartition theorem. Dashed lines are polynomial fits as a guide.

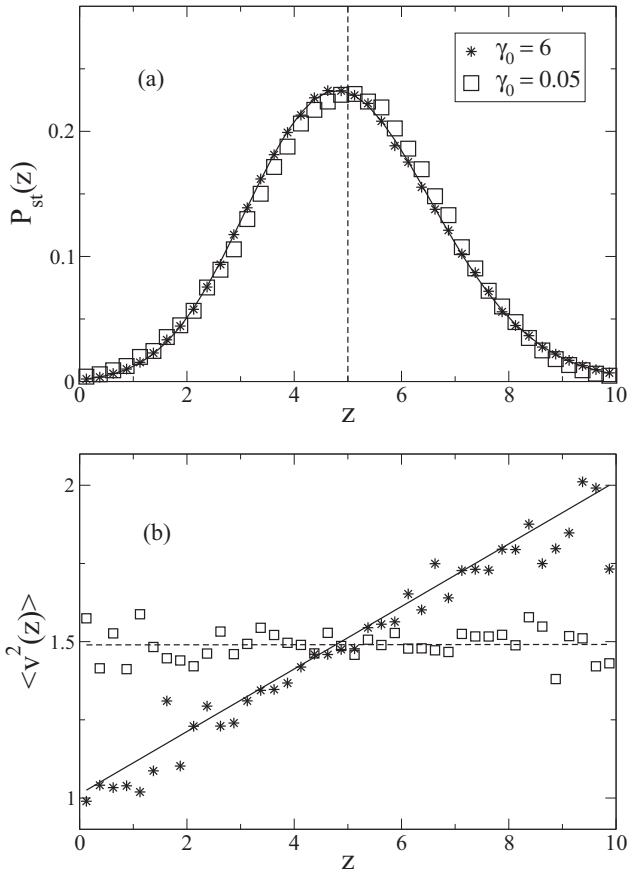

FIG. 2. (a) Simulation results of the steady distribution $P_{st}(z)$ for the harmonic potential. Simulation data (symbols) and the continuous line is the analytical expression (30). (b) Local second moment $\langle v^2(z)\rangle$ for the harmonic potential. Continuous line corresponds to the energy equipartition theorem (13), and the dashed line is a guide.

distribution,

$$P^u_{st}(v,\langle\hat{T}\rangle) = \frac{1}{\sqrt{2\pi\langle\hat{T}\rangle}} \exp\left[-\frac{v^2}{2\langle\hat{T}\rangle}\right]. \tag{26}$$

This fact will be analyzed in the discussion section.

B. Particle in harmonic potential

The following Langevin equation is proposed,

$$m\ddot{x} = -\gamma_0\dot{x} - k(x - 5x_0) + \sqrt{\gamma_0 k_B T_0 \hat{T}(x/x_0)}\,\eta(t), \tag{27}$$

with a trap at the center of the domain. After the changes (21), this equation transforms into the dimensionless form (1),

$$\ddot{z} = -\hat{\gamma}_0\dot{z} - \hat{k}(z - 5) + \sqrt{\hat{\gamma}_0\hat{T}(z)}\,\eta(\tau), \tag{28}$$

with the new stiffness dimensionless parameter,

$$\hat{k} = \frac{kx_0^2}{k_B T_0} = 0.5. \tag{29}$$

The overdamped steady distribution (9) is,

$$P^o_{st}(z) = N \exp\left[-\frac{\hat{k}z}{0.1} + \frac{\hat{k}(1 + 0.5z)}{0.01}\ln(1 + 0.1z)\right], \tag{30}$$

with the normalization constant $N = 0.00155$.

In Fig. 2(a) numerical results for the steady distribution $P_{st}(z)$ are plotted for two values of $\hat{\gamma}_0$, which are compared with the overdamped theoretical prediction. We see that the distribution $P^o_{st}(z)$ (30) is fulfilled for large enough friction but it presents small deviations as friction is reduced. The difference is not as large as in the former case due to confinement power of the potential.

In Fig. 2(b) numerical results for the energy equipartition theorem are plotted. Here we see also important deviations for low friction. Larger statistical dispersion is observed near the boundaries, because few particles are there due to the potential.

C. Particle in a two wells potential

The Langevin equation is now,

$$m\ddot{x} = -\gamma_0\dot{x} - \frac{V_0}{x_0} f(x/x_0) + \sqrt{\gamma_0 k_B T_0 \hat{T}(x/x_0)}\eta(t). \tag{31}$$

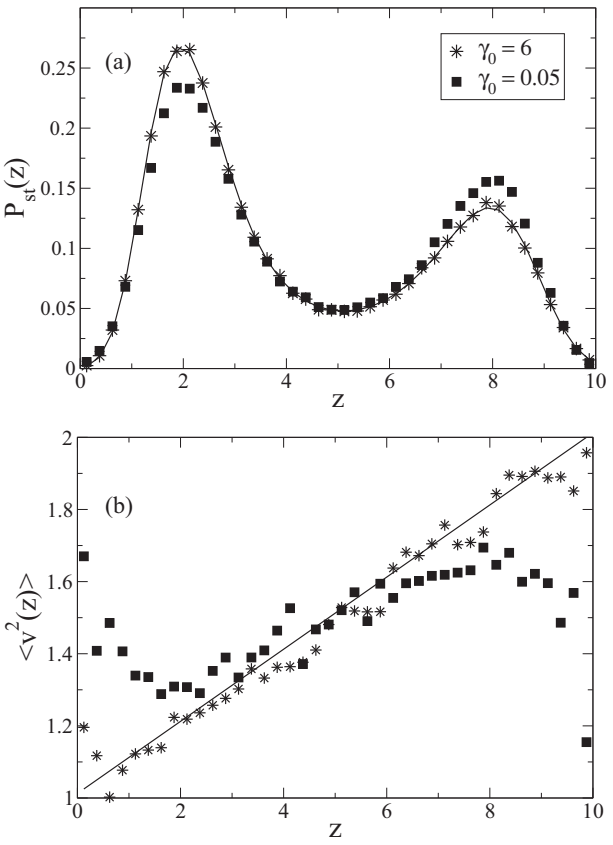

FIG. 3. (a) Simulation results of the steady distribution $P_{st}(z)$ for the bistable system. Simulation data (symbols). Continuous line is the numerical calculation of (9) for this system. (b) Local second moment $\langle v^2(z)\rangle$ for the values of previous figure. Continuous line corresponds to the energy equipartition theorem (13).

Using the same changes (21) we get the dimensionless equation,

$$\ddot{z} = -\hat{\gamma}_0 \dot{z} - \hat{V}_0 f(z) + \sqrt{\hat{\gamma}_0 \hat{T}(z)}\eta(\tau), \tag{32}$$

where the dimensionless force has been fixed,

$$\hat{V}_0 = \frac{V_0}{k_B T_0} = \frac{1}{250},$$
$$f(z) = (z-2)(z-5)(z-8), \tag{33}$$

which presents two symmetric steady stable states at $z = 2,8$ and an unstable one at the center $z = 5$.

Numerical results for the steady distribution are presented in Fig. 3(a). For large values $\hat{\gamma}_0 > 1$, the agreement with the overdamped solution is perfect, where the asymmetry of the two peaks is due to the temperature gradient. Deviations are observed in the underdamped regime which goes in the direction to restore the potential symmetry. As in the previous model this differences are no too large due to the effect of the potential. The energy equipartition theorem presents the same deviations than in former examples as can be see in Fig. 3(b).

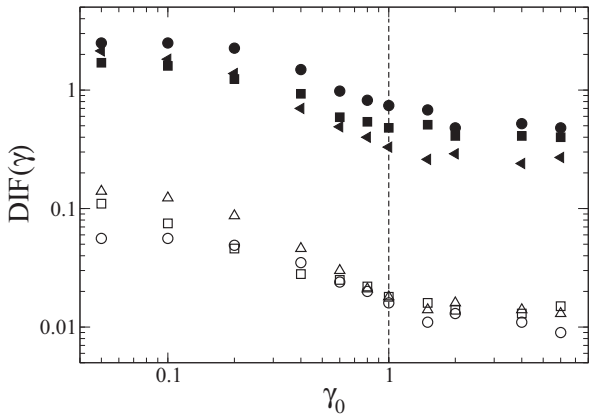

FIG. 4. Simulation results for the difference functions (18) and (19) in a log-log plot. Vertical dashed line separates the two regimes.

IV. DISCUSSION

It is worth discussing here two important results. The first one is the analysis of the quantified simulation data corresponding to the deviations between the underdamped and overdamped regimes. In Fig. 4 the quantities defined in (18) and (19) are plotted versus the friction parameter $\hat{\gamma}_0$. These deviations saturate in both underdamped and overdamped limits. It is clear that the separation between the underdamped and overdamped regimes occurs at the proposed value $\hat{\gamma}_0 \simeq 1$ (15).

The second result is the local violation of the energy equipartition theorem observed in the underdamped regime. Different spatial scales have to be considered to analyze this problem: the system size $\hat{L}_0 = 10$, the temperature gradient scale $\hat{l}_T = 10$, and the potential spatial range $\hat{l}_F$, which depends on the model. Friction incorporates also another length scale. In the underdamped regime the velocity has a large time scale $\tau_v = \hat{\gamma}_0^{-1}$, which allows particles to explore domains with different temperature without changing its velocity. When the space covered by a particle with a thermal velocity $v \sim \sqrt{\hat{T}}$ is of order $\hat{l}_T = 10$, then particles do not feel the local temperature and the equipartition theorem is violated locally. With our numbers this situation will appear for $\hat{\gamma}_0 \lesssim 0.1$.

The relevance of the friction is more reduced when a confined potential is present if $\hat{l}_F < \hat{l}_T$. In the last two examples one can see that for the harmonic potential $\hat{l}_F \simeq 2 < \hat{l}_T$ and for the two wells potential $\hat{l}_F \simeq 1 < \hat{l}_T$. In these two cases most particles are confined and they feel the local temperature of their minima.

V. CONCLUSIONS AND PERSPECTIVES

The study of the motion of Brownian particles under temperature gradient has been presented. We have analyzed the problem of the stochastic interpretation. The conclusion is that the Itô prescription is the most simple from computational requirements.

Nonequilibrium state distributions for the overdamped regime were checked satisfactorily by numerical simulations. Actually, it was shown that in the overdamped regime local equilibrium is also fulfilled. With respect the underdamped regime, without any possible analytical prediction,

numerical results show important deviations with the overdamped regime. In the case of free particles both steady distributions $P_{st}(z), P_{st}(v)$ evolve to a constant, indicating that temperature gradient has been averaged. Moreover, in this regime the local energy equipartition theorem is lost, and particles feel the averaged temperature. In those cases with confining potentials, the deterministic forces dominate and small corrections appear in $P_{st}(z)$, and the local energy equipartition theorem presents small deviations.

Finally, a condition for the separation of both underdamped and overdamped regimes $\hat{\gamma}_0 = 1$, has been checked and quantified by numerical simulations. On this result it is worth to comment the general case of a spatially dependent friction. Although the friction coefficient is indeed temperature dependent, it is not a very strong dependence, and accordingly the whole system has to be either in the underdamped or in the overdamped regime. For these reasons and in order to emphasize more the relevance of the nonequilibrium results a constant friction has been used. These results can be useful in experiments with colloids and traps in temperature and friction gradients [7,9,10].

ACKNOWLEDGMENTS

We acknowledge financial support from projects FIS2012-37655-C2-02 (Ministerio de Economía y Competitividad of Spain). Fruitful discussions with Professor L. Ramírez–Piscina are acknowledged.

[1] H. Risken, Z. Physik B **40**, 343 (1981).
[2] J. M. Sancho, M. San Miguel, and D. Dürr, J. Stat. Phys. **28**, 291 (1982).
[3] N. G. Van Kampen, Z. Phys. B **68**, 135 (1987).
[4] S. H. Lee and D. G. Grier, Phys. Rev. Lett. **96**, 190601 (2006).
[5] A. W. C. Lau and T. C. Lubensky, Phys. Rev. E **76**, 011123 (2007).
[6] C. López and U. Marini Bettolo Marconi, Phys. Rev. E **75**, 021101 (2007).
[7] G. Volpe, L. Helden, T. Brettschneider, J. Wehr, and C. Bechinger, Phys. Rev. Lett. **104**, 170602 (2010).
[8] T. Brettschneider, G. Volpe, L. Helden, J. Wehr, and C. Bechinger, Phys. Rev. E **83**, 041113 (2011).
[9] S. Duhr and D. Braun, Phys. Rev. Lett. **96**, 168301 (2006).
[10] J. N. Pedersen, Ch. J. Lüscher, R. Marie, L. H. Thamdrup, A. Kristensen, and H. Flyvbjerg, Phys. Rev. Lett. **113**, 268301 (2014).
[11] R. Mannella and P. V. E McClintock, Phys. Rev. Lett. **107**, 078901 (2011).
[12] J. M. Sancho, Phys. Rev. E **84**, 062102 (2011).
[13] S. Hottovy, G. Volpe, and J. Wehr, J. Stat. Phys. **146**, 762 (2012).
[14] G. Pesce, A. McDaniel, S. Hottovy, J. Wehr, and G. Volpe, Nat. Commun. **4**, 2733 (2013).
[15] A. Celani, S. Bo, R. Eichhorn, and E. Aurell, Phys. Rev. Lett. **109**, 260603 (2012).
[16] M. Yang and M. Ripoll, Phys. Rev. E **87**, 062110 (2013).
[17] M. Polettini, Phys. Rev. E **87**, 032126 (2013).
[18] X. Durang, Ch. Kwon, and H. Park, Phys. Rev. E **91**, 062118 (2015).
[19] T. Kuroiwa and K. Miyazaki, J. Phys.: Math. Theor. **47**, 012001 (2014).
[20] O. Farago and N. Grønbech-Jensen, Phys. Rev. E **89**, 013301 (2014).
[21] F. Sagués, J. M. Sancho, and J. García-Ojalvo, Rev. Mod. Phys. **79**, 829 (2007).
[22] A. M. Lacasta, J. M. Sancho, A. H. Romero, I. M. Sokolov, and K. Lindenberg, Phys. Rev. E **70**, 051104 (2004).
[23] T. C. Gard, *Introduction to Stochastic Differential Equations* (Dekker, New York, 1987).